Supporting Information

Highly ordered $ZnMnO_3$ nanotube arrays from "self-sacrificial" ZnO template as high-performance electrodes for lithium ion batteries

Hongbin Chen, Liang-Xin Ding,* Kang Xiao, Sheng Dai,

Suqing Wang and Haihui Wang*

School of Chemistry & Chemical Engineering, South China University of Technology, Guangzhou 510640, China.

School of Chemical Engineering, The University of Adelaide, SA 5006, Adelaide, Australia.

1. Experimental section

1.1 Preparations of $ZnMnO_3$ NTAs on nickel foam

All chemical reagents were analytical (AR) grade and purchased without any further purification. Electrochemical deposition proceeds in a two-electrode electrolyzer via galvanostatic electro-deposition, and the graphite electrode was used as a counter electrode. Nickel foam as a working electrode. ZnO nanorods arrays (ZnO NRAs) template was electrodeposited in solution of 0.01 M $Zn(NO_3)_2$ and 0.05 M NH_4NO_3 at a current density of 1.5 $mA \cdot cm^{-2}$ at 70 °C for 90 min. Then, the ZnO@$ZnMnO_3$-precusors core-shell NTAs were obtained by electro-deposition of nanoparticles on the surfaces of ZnO nanorods in solution of 0.01 M $Mn(CH_3COO)_2 \cdot 4H_2O$ and 0.02 M CH_3COONH_4 with current density of -0.25 $mA \cdot cm^{-2}$ at 70 °C for 20 min. Then the as-prepared sample was placed into a tube furnace under argon air at the temperature 300 °C for 300 min. The ZnO@$ZnMnO_3$-precusors core-shell NTAs were fabricated.

The prepared ZnO@$ZnMnO_3$-precusors core-shell NTAs were immersed in ammonia solution for 12 h to completely dissolved the residual ZnO NRAs template, and eventually the $ZnMnO_3$ NTAs were obtained.

1.2 Material characterization

The microstructure of $ZnMnO_3$ NTAs was characterized by scanning electron microscopy (SEM) (Quanta 200F) and transmission electron microscopy (TEM) (FEI, Tecnai G2 F30 S-Twin). The elements and chemical formula were tested by X-ray diffraction (XRD) (Bruck D8 Advance). The elemental component was tested by energy dispersive X-ray analyzer (EDX) (X-MaxN20). The elements and valence state of the surface of samples was investigated by X-ray photoelectron spectroscopy (XPS) (ESCALAB250).

1.3 Electrochemical measurements

The electrochemical properties were investigated based on coin cells (CR2025). The celgard (2325) membrane was used as the separator between cathode and anode. The electrolyte solution consisted of $LiPF_6$, ethylenecarbonate and diethylcarbonate.1 M $LiPF_6$ dissolved in blend of 500 mL ethylenecarbonate and 500 mL diethylcarbonate. Analytical grade lithium plate was assembled as the cathode and $ZnMnO_3$ NTAs were the anode. The coin cells were assembled and installed in an inert atmosphere (Ar) in glove-box (Mikrouna, super 1220) where a constant amount of oxygen and moisture less than 1 ppm. The galvanostantic charge and discharge of the coin cells were processed on a multi-channel battery testing device (Neware Electronic Co., China)in the voltage range from 0.01-3.0 V at constant temperature of 25 °C. Cycle voltammetry (CV) and electrochemical impedance spectra (EIS) of the coin cells were processed by electrochemical workstation (Zahner IM6ex) at a scanning rate of 0.2 mV s^{-1}.

2. Supplementary figures and tables

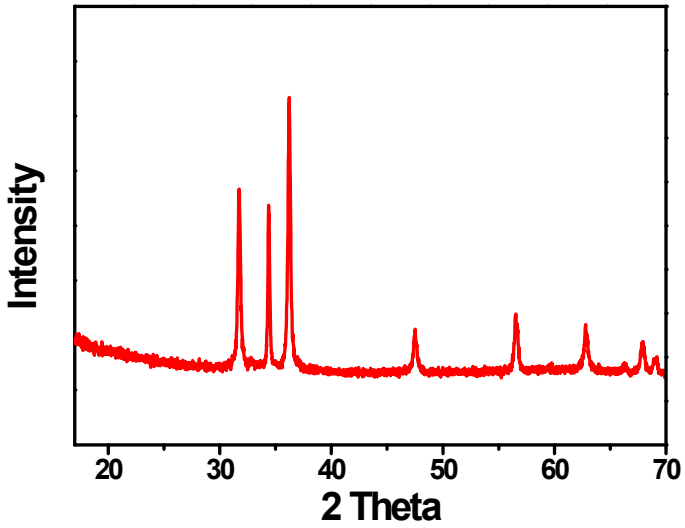

Fig. S1 XRD pattern of ZnO template.

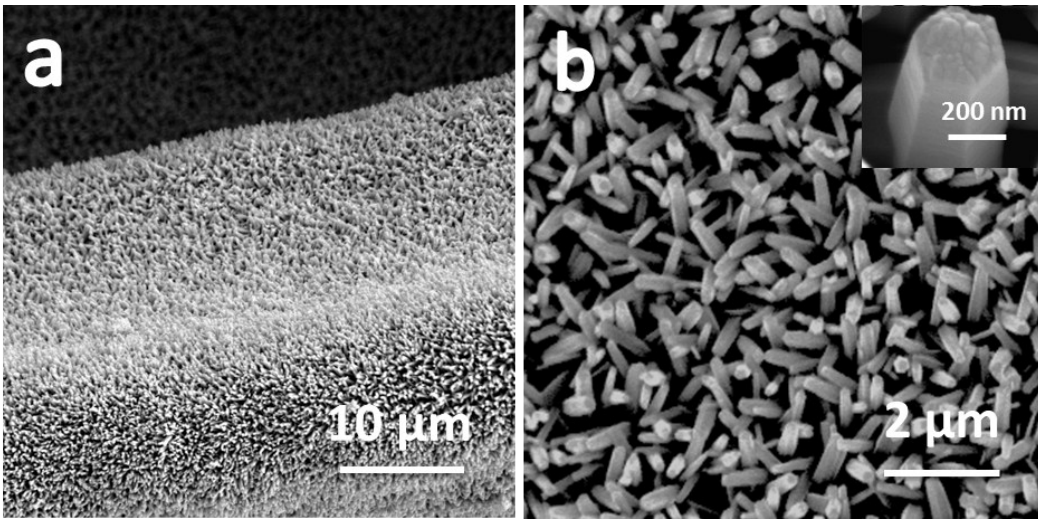

Fig. S2 (a-b) SEM images of ZnO nanorods on nickel foam substrate.

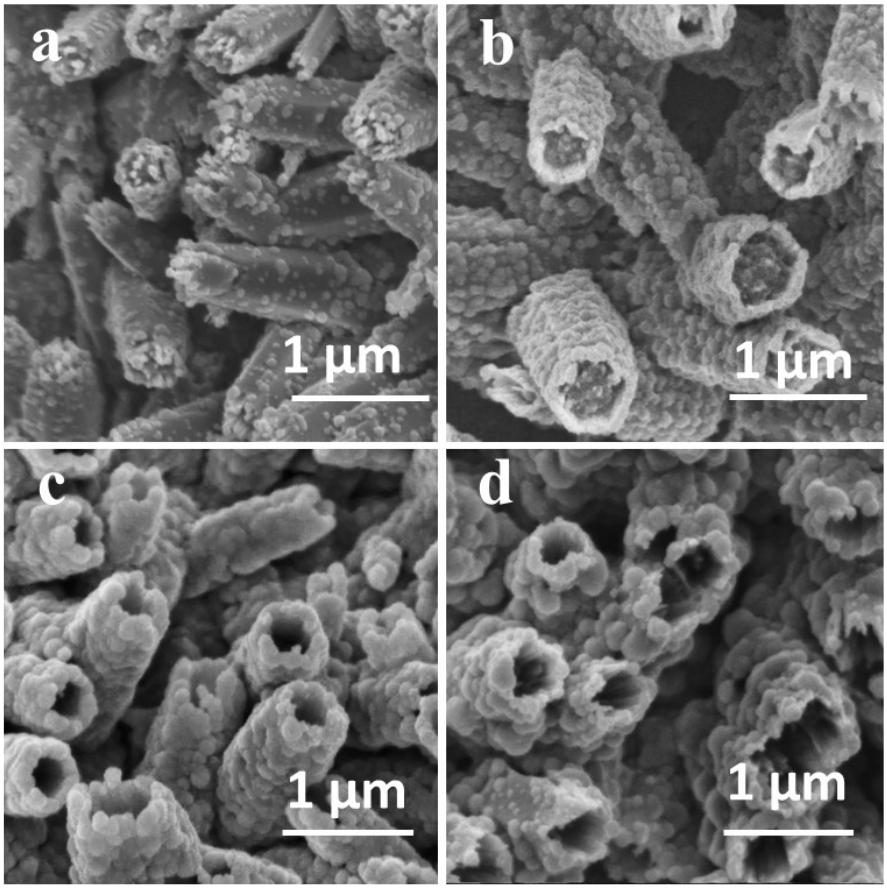

Fig. S3 SEM images of ZnO@$ZnMnO_3$-precursors with different electro-position times of (a) 5 min, (b) 10 min, (c) 20 min and (d) 25 min.

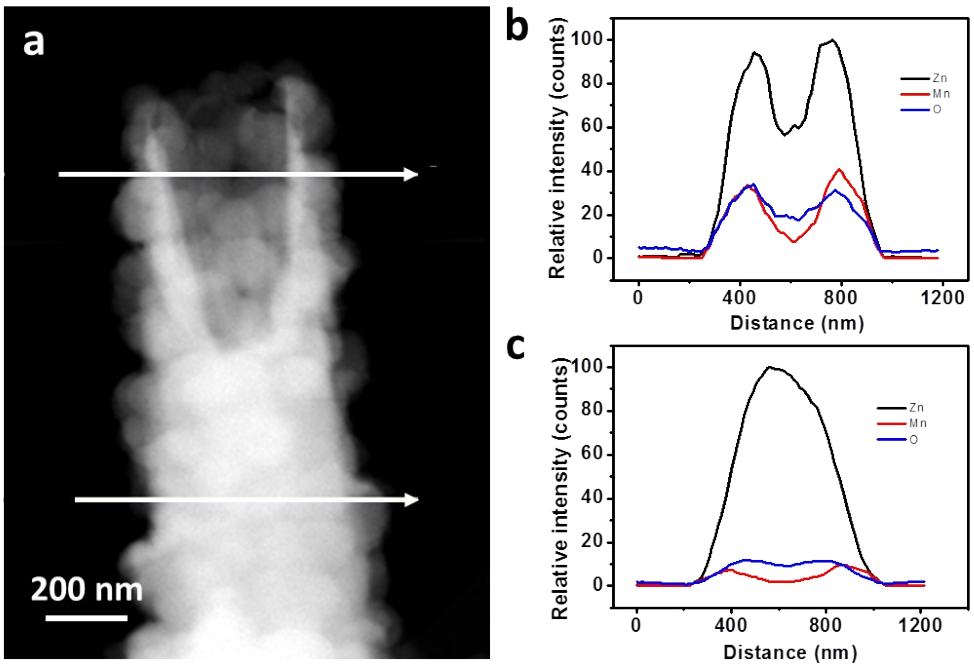

Fig. S4 (a) STEM of ZnO@$ZnMnO_3$-precursors core-shell nanorod with electro-deposition time of 20 min before dissolution of ZnO; (b,c) EDX line scans of different position of ZnO@$ZnMnO_3$-precursors.

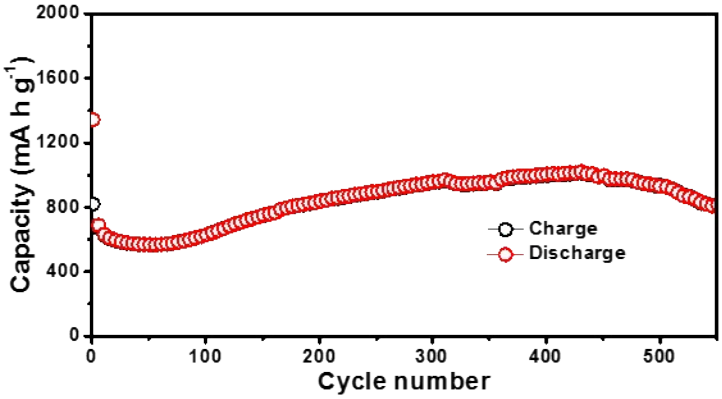

Fig. S5. Long cycling performance of $ZnMnO_3$ at a current density of 500 mA g^{-1}.

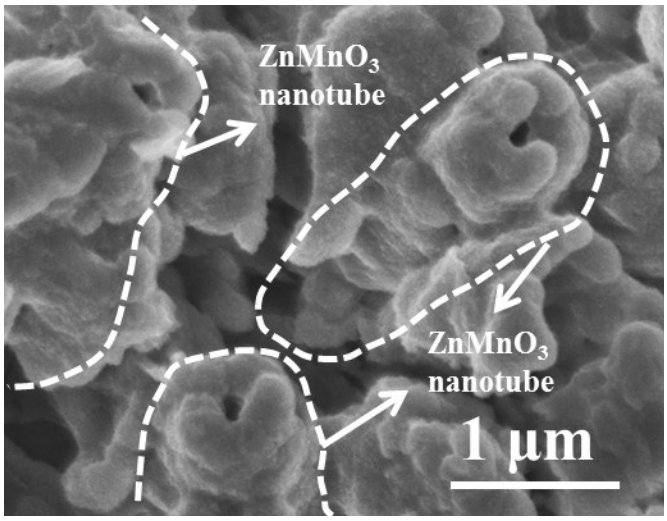

Fig. S6 SEM image of the $ZnMnO_3$ NTAs after 200 cycles.

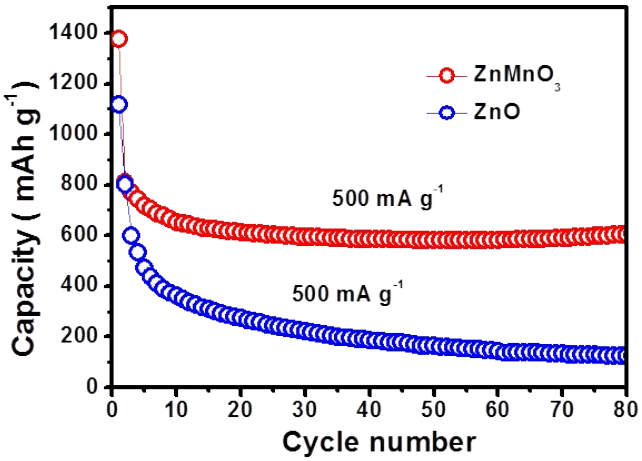

Fig. S7 Cycling performance of the $ZnMnO_3$ NTAs and the ZnO NRAs.

Table S1 Comparison of $ZnMnO_3$ NTAs versus several kinds of MOMTs for LIBs.

Materials	Cycling performance	Rate performance	Reference
$ZnMnO_3$ NTAs	858mAh g^{-1} at 500 mA g^{-1}after 200 cycles (capacity rising duringthecycling). 99% capacity retention	827mA g^{-1} at 100mA g^{-} 701mA g^{-1} at 200mA g^{-1} 466mA g^{-1} at 1000mA g^{-1} 364mA g^{-1} at 2000mA g^{-1} 208mA g^{-1} at 5000mA g^{-1}	This work
$ZnMn_2O_4$ ball-in-ball	750 mAh g^{-1} at 400 mA g^{-1}after120 cycles(capacity rising duringthecycling).99% capacity retention	683 mA g^{-1} at 600 mA g^{-1} 618mA g^{-1} at 800mA g^{-1} 480mA g^{-1} at 1000mA g^{-1} 396mA g^{-1} at 1200mA g^{-1}	[1]
Double-shelled $CoMn_2O_4$	624mAh g^{-1} at 200 mA g^{-1} after50 cycles.76% capacity retention	624mA g^{-1} at 200 mA g^{-1} 515mA g^{-1} at 515mA g^{-1}	[2]
$NiCo_2O_4$nanotubes	590mAh g^{-1} at 100 mA g^{-1}after200 cycles.59% capacity retention	590mA g^{-1} at 100 mA g^{-1} 273mA g^{-1} at 5000mA g^{-1}	[3]
Porous $Ni_xCo_{3-x}O_4$	844mAh g^{-1}at 500 mA g^{-1}after200 cycles(capacity rising duringthecycling).99% capacity retention	1331mA g^{-1} at 100 mA g^{-1} 736mA g^{-1} at 200mA g^{-1} 589mA g^{-1} at 400mA g^{-1} 545mA g^{-1} at 800mA g^{-1} 293mA g^{-1} at 1600 mA g^{-1}	[4]
CoV_2O_6nanosheets	702mAh g^{-1} at 200 mA g^{-1}after200 cycles.88% capacity retention	435mA g^{-1} at 200mA g^{-1} 581mA g^{-1} at 5000 mA g^{-1}	[5]
$CoMo_2O_4$nanosheets	894 mAh g^{-1} at 100 mA g^{-1}after100 cycles.88% capacity retention	1008mA g^{-1} at 200mA g^{-1} 996mA g^{-1} at 300mA g^{-1} 918mA g^{-1} at 500mA g^{-1} 778mA g^{-1} at 1000mA g^{-1} 611mA g^{-1} at 1500mA g^{-1}	[6]
$NiCo_2O_4$ spheres	706 mAh g^{-1} at 200 mA g^{-1}after100 cycles.78% capacity retention	834mA g^{-1} at 300mA g^{-1} 745mA g^{-1} at 600mA g^{-1} 662mA g^{-1} at 1000mA g^{-1} 533mA g^{-1} at 2000mA g^{-1}	[7]
$ZnFe_2O_4$microrods	542mAh g^{-1}at 1000 mA g^{-1} at 488th cycles(capacity rising duringthecycling).100% capacity retention	1141mA g^{-1} at 100mA g^{-1} 781mA g^{-1} at 250mA g^{-1} 481mA g^{-1} at 500mA g^{-1} 416mA g^{-1} at 1000mA g^{-1} 326mA g^{-1} at 1500mA g^{-1}	[8]

Reference

[1] G. Zhang, L. Yu, H. B, Wu, H. E. Hoster, X. W. Lou, *Adv. Mater.*,2012, **24**, 4609-4613.

[2] L. Zhou, D. Zhao, X. W. Lou, *Adv. Mater.*, 2012, **24**, 745-748.

[3] J. Zhu, Z. Xu, B. Lu, *Nano Energy*, 2014, **7**, 114-123.

[4] F. Zheng, D. Zhu, Q. Chen, *ACS Appl. Mater. Interfaces*, 2014, **6**, 9256-9264.

[5] L. Zhang, K, Zhao, Y. Lou, Y. Dong, M. Yan, W. Ren, L. Zhou, L. Qu, L. Mai, *ACS Appl. Mater. Interfaces*, 2016, **8**, 7139-7146.

[6] H. Yu, C. Guan, X. Rui, B. Ouyang, B. Yadian, Y. Huang, H. Zhang, H.-E, Hoster, H.-J. Fan, Q, Yan, *Nanoscale*, 2014, **6**, 10556-10561.

[7] L. Shen, L. Yu, X. -Y. Yu, X. Zhang, X. W. Lou, *Angew. Chem. Int. Ed*., 2015, **54**, 1868-1872.

[8] L. Hou, H. Hua, L. Lian, H. Cao, S. Zhu, C. Yuan, *Chem. Eur. J.*, 2015, **21**, 13012-13019.